



Coastline responses to changing storm patterns

Jordan M. Slott,^{1,2} A. Brad Murray,^{1,2} Andrew D. Ashton,³ and Thomas J. Crowley^{1,2}

Received 3 July 2006; revised 9 August 2006; accepted 14 August 2006; published 20 September 2006.

[1] Researchers and coastal managers are pondering how accelerated sea-level rise and possibly intensified storms will affect shorelines. These issues are most often investigated in a cross-shore profile framework, fostering the implicit assumption that coastline responses will be approximately uniform in the alongshore direction. However, experiments with a recently developed numerical model of coastline change on a large spatial domain suggest that the shoreline responses to climate change could be highly variable. As storm and wave climates change, large-scale coastline shapes are likely to shift—causing areas of greatly accelerated coastal erosion to alternate with areas of considerable shoreline accretion. On complex-shaped coastlines, including cusped-cape and spit coastlines, the alongshore variation in shoreline retreat rates could be an order of magnitude higher than the baseline retreat rate expected from sea-level rise alone. **Citation:** Slott, J. M., A. B. Murray, A. D. Ashton, and T. J. Crowley (2006), Coastline responses to changing storm patterns, *Geophys. Res. Lett.*, 33, L18404, doi:10.1029/2006GL027445.

1. Introduction

[2] Warming of the atmosphere and oceans expected in coming decades [*Intergovernmental Panel on Climate Change*, 2001] will likely cause storm behavior to change. Although changes in storminess cannot currently be predicted with complete confidence, there is good reason to expect some change in extra-tropical and tropical cyclone frequency and severity [*Emanuel*, 1987, 2005; *Lambert*, 1995; *Geng and Sugi*, 2003; *Webster et al.*, 2005]. (Recent work suggests that the total energy dissipated by tropical storms from meteorological records has doubled over the past 30 years, and furthermore, is well-correlated with the observed 0.5°C rise in SSTs [*Emanuel*, 2005]). Shifts in storm behavior will alter the amounts of wave energy approaching a shore from different directions (the ‘wave climate’). Previous studies using a numerical model of coastline change on a large spatial domain [*Ashton et al.*, 2001; *Ashton and Murray*, 2006a, 2006b] have shown that distinct plan-view shoreline shapes (e.g. cusps, spits) can emerge and evolve under different wave climates. Therefore, if storm patterns and wave distributions change, coastline shapes will tend to adjust—a process involving greatly accelerated shoreline

erosion in many areas that would affect coastal communities and infrastructure.

[3] Shoreline changes from sea-level rise have received considerable attention [*Anderson et al.*, 2001; *Brown et al.*, 2004; *Bruun*, 1962; *Cowell et al.*, 1995; *Gornitz*, 1991; *Titus et al.*, 1991; *Zhang et al.*, 2000, 2004] (see also U.S. Climate Change Science Program, Potential consequences of climate variability and change on coastal areas and marine resources, 2001, available at www.usgcrp.gov/usgcrp/nacc/coasts/default.htm). Many studies assume that on sandy coastlines, sea-level rise causes cross-shore sediment redistribution that leads to a landward translation of the shoreline [*Bruun*, 1962; *Cowell et al.*, 1995; *Zhang et al.*, 2000, 2004]. Under this conceptual framework, shorelines will retreat in a roughly alongshore-uniform manner in response to global warming. In contrast, we evaluate here the heterogeneous nature of shoreline retreat related to changing storm patterns on time scales of decades to centuries.

[4] We use a numerical model to explore how a rapid change in wave climate will affect a cusped coastline shape, similar to the shape of the Carolina Capes, from Cape Hatteras, NC to Cape Fear, SC, USA (Figure 1). This region of coastline serves as an important and illustrative case study. Many parts of the Carolina Capes are heavily developed and economically important; accelerated rates of shoreline migration will further threaten homes and businesses built near the shoreline there today [*Pilkey et al.*, 1998]. We conducted two sets of model experiments, and in each compare coastline changes under altered wave climates with coastline changes under the current wave climate off of the Southeast US Coast. In the first set, we select several representative wave climate-change scenarios, based on an estimate of how storminess might change in the future. In the second set of model experiments, we expand the number of model runs to include a wider range of possible future wave climates.

2. Methods

2.1. Numerical Model

[5] We first briefly discuss the model we use for this evaluation, which has been described previously [*Murray and Ashton*, 2004; *Ashton et al.*, 2001]. When waves break at a shoreline, they drive a flux of sediment along the shore. The magnitude of this flux is related to the breaking-wave height, and to the wave approach angle, relative to the shoreline orientation (Figure 2). Alongshore sediment fluxes, Q_s , are based on the commonly used CERC equation [*Komar and Inman*, 1970; *Komar*, 1998]:

$$Q_s = K_1 H_b^{5/2} \sin(\phi_b - \theta) \cos(\phi_b - \theta), \quad (1)$$

where H_b and ϕ_b are breaking-wave height and crest angle, respectively, and θ is local shoreline orientation. K_1 is an

¹Division of Earth and Ocean Sciences, Nicholas School of the Environment and Earth Sciences, Duke University, Durham, North Carolina, USA.

²Also at Center for Nonlinear and Complex Systems, Duke University, Durham, North Carolina, USA.

³Woods Hole Oceanographic Institution, Woods Hole, Massachusetts, USA.

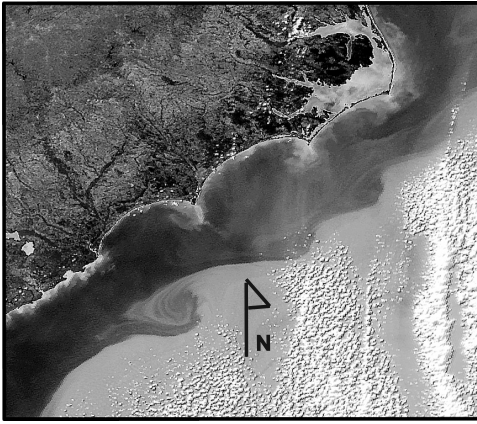


Figure 1. Satellite image of the Carolina capes. The Carolina capes, along the US Southeastern coast, from Cape Hatteras, NC to Cape Fear, SC, USA, courtesy of the SeaWiFS Project NASA/GSFC and ORBIMAGE.

empirical constant equal to $0.4 \text{ m}^{1/2}/\text{s}$ for the sandy coastline considered here (as discussed in Section 4).

[6] On a sandy coastline, alongshore gradients in this sediment flux, Q_s , tend to cause changes in the shoreline position, η (Figure 2):

$$\partial\eta/\partial t = -(1/D)\partial Q_s/\partial x, \quad (2)$$

where D is the seabed depth to which erosion or accumulation extends. Large-scale ($> \text{km}$) bends in a shoreline cause gradients in alongshore flux that alter the shoreline shape. When waves approach from nearly straight offshore (as measured in deep-water, before nearshore refraction), gradients in alongshore transport cause the large-scale shoreline shape to become smoother (Figure 2a). However, when waves approach from deep-water angles greater than approximately 45° ('high-angle' waves, greater than the deep-water angle at which alongshore sediment transport is maximized), plan-view shoreline undulations grow [Ashton *et al.*, 2001] (Figure 2b). Where high-angle waves dominate regional wave climates, complex coastline shapes and behaviors arise [Ashton *et al.*, 2001]. In a recently developed numerical model based on (1) and (2) different shapes including cusped capes and spits evolve under different wave distributions (characterized by the proportions of high-

angle versus low-angle waves, and by the degree of asymmetry—the proportion of wave influence from the left versus right, looking offshore) [Ashton *et al.*, 2001].

[7] The model domain is discretized into cells, and shoreline changes are determined by a discretized form of (equation 2). Where protruding shoreline features block other coastline segments from the current deep-water wave-approach angle, no sediment transport occurs in the 'shadowed' segments. A new deep-water wave angle is chosen daily from a probability distribution function (PDF) that represents a wave climate. Breaking-wave height and angle relative to local shoreline orientations are calculated assuming refraction and shoaling over shore-parallel contours.

2.2. Representing the Recent Wave Climate

[8] We use twenty years of wave hindcasts off of the North Carolina coast, USA (station 509) (WIS data can be found at <http://frf.usace.army.mil/wis/>, hereafter *WIS*) as our 'constant' wave climate representing recent conditions. We form the wave climate model input PDF from the wave hindcasts as follows. First, we rewrite the alongshore sediment transport formula (equation 1) above in terms of deep-water wave heights and angles by assuming that waves shoal and refract over shore-parallel contours [Ashton *et al.*, 2001]: $Q_s = K_2 H_o^{12/5} \sin(\phi_o - \theta) \cos^{6/5}(\phi_o - \theta)$, where H_o is the deep-water wave height, ϕ_o is the deep-water wave approach angle, and K_2 is an empirical constant equal to $0.32 \text{ m}^{3/5} \text{ s}^{-6/5}$. The influence a deep-water wave has on alongshore sediment transport, therefore, scales with the $12/5$ th power of its wave height. Next, we scale each wave height from the wave hindcasts (*WIS*) accordingly before being added to the wave approach angle PDF. We fit two parameters, A and U , to the PDF (e.g., Figure 3). The dimensionless wave-asymmetry parameter, A , describes the proportion of wave influences approaching from the left (looking off-shore); the dimensionless wave-angle highness parameter, U , describes the proportion of wave influences approaching from high-angles ($> \sim 45^\circ$). (Together, they describe four probability bins: from-the-left and high-angle, from-the-left and low-angle, from-the-right and low-angle, and from-the-right and high-angle.) Deep-water significant wave height is held constant at 1.7 m throughout each simulation, based on $\langle H_o^{12/5} \rangle^{5/12}$ for the hindcast data (*WIS*)—the effective average wave height for calculating net alongshore sediment transport.

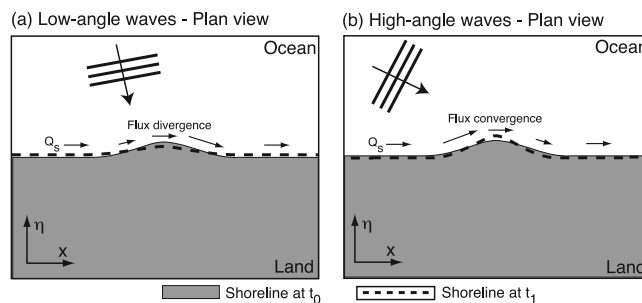


Figure 2. Schematic illustration of gradients in the magnitude of alongshore sediment flux, shown by the length of the arrows, caused by changes in shoreline orientation, and the consequent zones of erosion and accretion. (a) Erosion and the subsequent landward retreat of the plan-view 'bump' occurs under the influence of low-angle waves. (b) Accretion and the subsequent seaward build-out of the plan-view 'bump' occurs under the influence of high-angle waves.

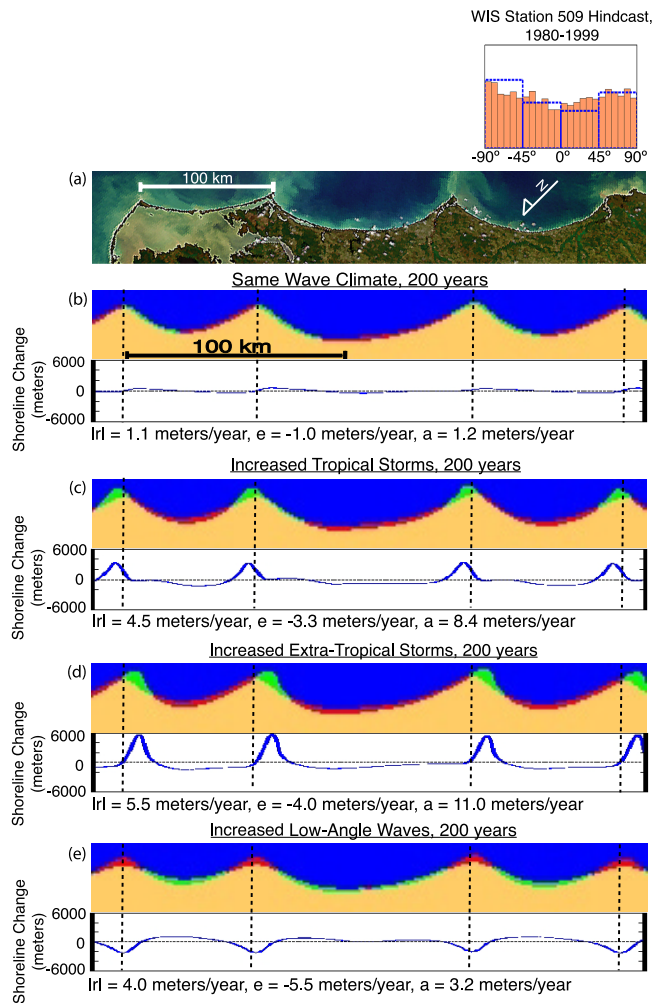


Figure 3. Plan-view shorelines. (a) The Carolina capes rotated counterclockwise 150 degrees so that the regional offshore direction is up, with a depiction of the regional wave climate (inset) showing relative wave influence from each 7.5° angle bin [Ashton *et al.*, 2003a, 2003b]. (b) Model shoreline shape produced using wave-climate parameters based on WIS station 509 off of North Carolina, USA (WIS): The proportion of high-angle waves, U , = 0.60; the proportions of waves from the left, A , = 0.55, and average deep-water wave height = 1.7m. The model wave climate is depicted by the blue bin outlines in the histogram. Also shown are the shoreline changes occurring over 200 years with this same wave climate; red indicates shoreline erosions, and green indicates accretion. The alongshore average of the magnitude of shoreline-change rates is denoted by $|r|$, the alongshore-averaged erosion (accretion) rates within eroding (accreting) shoreline segments are denoted by e (a). Shoreline change is also depicted graphically. (c) Initial coastline as in Figure 3b, modified over 200 years by a wave climate with U , = 0.70 and A , = 0.45. (d) Initial coastline as in Figure 3b, modified over 200 years by a wave climate with U , = 0.70 and A , = 0.65. (e) Initial coastline as in Figure 3b, modified over 200 years by a wave climate with U , = 0.50 and A , = 0.55. Satellite image courtesy of the SeaWiFS Project NASA/GSFC and ORBIMAGE.

2.3. Initial Conditions for Model Experiments

[9] To produce the initial coastline for model experiments (Figure 3b), we based the model wave climate roughly on the 20 years of wave hindcast off of the Carolina coast (WIS), and beginning with a straight shoreline (plus white-noise perturbations), let the model run for approximately 8000 simulated years. We treat this simulated coastline as a representative example of a cusped coast, rather than attempting to model the evolution and morphology of the Carolina coastline in detail. (The Holocene development of the Carolina Capes likely started with large-scale undulations in the inherited coastline, requiring less time than the evolu-

tion from an approximately straight coast in the model. In addition, wave climates have not likely been constant for millennia. We assume only that over recent centuries wave climates have been steady enough for such coastline shapes to attain a quasi-equilibrium.)

[10] Mid-latitude winter storms off of the US East Coast produce waves that tend to approach from the northeast at high-angles relative to the trend of the Carolina coastline (Figure 1), whereas Atlantic tropical storms produce waves from the south. These two storm influences combine to produce a regional wave climate dominated by high-angle waves, as well as a moderate asymmetry (net transport would

be to the southwest along a straight coastline with the overall trend of the Carolina Capes).

2.4. Changes in Wave-Climate Parameters for Varying Storm Activity

[11] To conduct experiments exploring the effects of changes in storm activity, we must first estimate a reasonable magnitude for changes in the model wave-climate parameters. Precisely how tropical storms, extra-tropical storms, and prevailing winds will change as the climate warms remains unknown. However, we use the predicted increase in tropical storminess as a guide, starting with *Emanuel's* [1987] prediction that tropical-storm wind speeds will increase by 10% given a 2° SST increase. Although we can reasonably expect that global warming will also lead to changes in storm frequency, duration, and size, we only consider a 10% increase in storm wind speed [Emanuel, 1987] as both a simplifying assumption and conservative estimate of change.

[12] An index of the shear stress exerted on the water surface by wind, u_a (m/s), is a non-linear function of the wind speed, u (m/s): $u_a = 1.7u^{1.23}$ [Komar, 1998]. Empirical measurements show that in situations where the distance over which the wind blows (fetch) limits the growth of the waves, wave heights scale linearly with u_a . However, if the fetch does not limit the growth of the waves, wave heights scale quadratically with u_a . If we increase the wind speed, u , by 10% these empirical relationships suggest wave height increases between ~12% (fetch-limited) and ~26% (fully-developed waves) [Komar, 1998]. In lieu of a fetch analysis of storm winds, we chose a 12% (fetch-limited) increase in wave heights as a conservative estimate. Using the 12/5th scaling relationship between deep-water wave height and alongshore sediment transport, a ~12% increase in the deep-water wave height (fetch-limited) results in an approximately 32% increase in alongshore sediment transport.

[13] For our Carolina coastline case study (Figure 1), the vast majority of waves generated by tropical storms approach the coast from the right (using a regionally-averaged coastline orientation). The approximation that all tropical-storm derived waves come from the right allows a simple calculation of a change in wave-climate asymmetry, A , starting from the estimated wave climate for the last two decades of last century (WIS), $A = 0.55$, $U = 0.60$.

[14] If we let E_{left} represent the wave-height influence on alongshore sediment transport from left-approaching waves and E_{right} represent the wave-height influence from right-approaching waves, the wave climate parameter, A , represents the proportion of left-approaching wave-height influences:

$$A = \frac{E_{left}}{E_{left} + E_{right}} \quad (3)$$

[15] Inserting $A = 0.55$ (the value representing the present wave climate) into equation 3, yields $E_{right} = 0.82 E_{left}$. Holding the wave-height influence from the left constant, and increasing the new E_{right} to $1.32(0.82) E_{left}$ (i.e. by 32%) leads to $A_{new} = 0.48$; a 12.7% change in the parameter value. Given the conservative fetch-limitation assumption, changing A from 0.55 to 0.45 seems reasonable. Based on this simple analysis, we use a 0.10 change as a reasonable order-

of-magnitude estimate for the changes in wave-climate parameters in all of the storm-change scenarios examined in the first set of model experiments described in the next section.

3. Results

[16] We conducted a sensitivity study to investigate the responses of a cusped coastline to several climate change scenarios. Figure 3b shows the changes in the model coastline over 200 years of evolution under a constant wave climate; the large-scale coastline shape changes relatively little on human timescales under these conditions, although continued southwestward translation of the capes does cause shoreline changes of hundreds of meters per century near the capes, consistent with historical observations (Fifty-year historical shoreline data for North Carolina can be found at <http://dcm2.enr.state.nc.us/Maps/erosion.htm>, hereafter NC50).

[17] Figure 3c shows how the simulated coastline changes during 200 years of evolution under an altered wave climate ($A = 0.45$, $U = 0.70$) that corresponds to an increase in the influence of tropical-storm waves approaching from the south. (Atlantic tropical storms, as they propagate toward and along the Southeast US coastline, radiate waves toward the Carolina coastline from highly oblique angles.) Figure 3d shows the effects from an increased influence of extra-tropical storms ($A = 0.65$, $U = 0.70$), with more waves approaching from the north and east. For comparison, Figure 3e shows the effects of a 0.10 decrease only in U , which would occur along the Carolina Coast if the relative energy from tropical and extra-tropical storms decreased (caused for example by an increase in onshore breezes). In addition to affecting the wave approach angle distributions, we would also expect the average wave height to increase (decrease) as a result of increased (decreased) storminess. For simplicity, however, we do not change the average wave height (1.7 m) used in these model runs.

[18] In the wave-climate-change scenarios, areas of accretion as well as large areas of accelerated erosion result, with alongshore-averaged shoreline change rates (including magnitudes of erosion and accretion rates individually) several times those that occurred without the change in wave climate. Maximum shoreline-change rates in the climate-change scenarios (Figures 3c–3e) approach an order of magnitude higher than the maximum rates with the unchanged climate (Figure 3b). In increased-storminess scenarios (Figures 3c and 3d), accretion concentrates near the cape tips and ranges between 8 and 11 meters/year, while erosion spans the cusped bays with rates of 3–4 m/yr. Under the decreased storminess scenario, cape tips erode at roughly 5.5 m/yr, while the cusped bays accrete at roughly 3.2 m/yr.

[19] The changes in wave-climate-parameters of 0.10, suggested by the calculations in Section 2.3, are not expected to represent future wave-climate changes with a high degree of accuracy. We have also conducted a large number of simulations with a range of changes in wave-climate parameters to more fully explore the possible range of coastline responses. Figure 4 shows the alongshore-averaged shoreline change and erosion rates that result in the model from different combinations of changes in wave-climate parameters. The dotted rectangle (Figures 4a,b) encloses the region

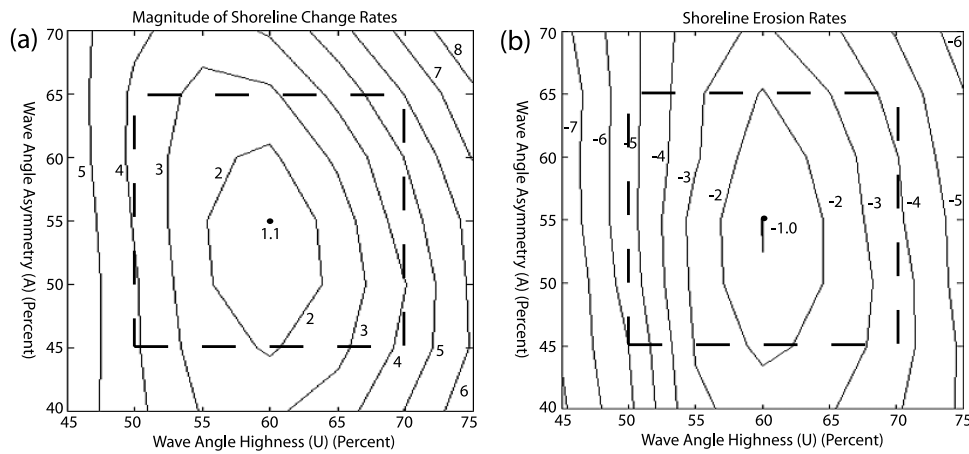


Figure 4. Contour plots of shoreline-change and erosion rates (meters/year) for different combinations of wave climate parameters A and U , in experiments like those described in Figure 3. The rates under an unchanged climate ($A = 0.55$, $U = 0.60$) are marked with small filled circles. (a) Alongshore-averaged magnitude of shoreline change, $|r|$ (m/yr). (b) Alongshore-averaged erosion within eroding coastline segments, e (m/yr). The dashed rectangles delineate the regions where the wave climate changes at most by 0.10 in each or both of the wave climate parameters.

representing wave-climate-parameter changes of at most 0.10, which we might conservatively expect over the coming decades to centuries. Along the edges of this rectangle, rates of shoreline change (Figure 4a) range from roughly 2 to 6 m/yr (compared to 1.1 m/yr for the current wave climate), while erosion rates (Figure 4b) range from roughly 2 to 5 m/yr (compared to 1.0 m/yr for the current wave climate). The lower-right (upper-right) vertices of the rectangle represent the experiments depicted by (Figures 3c (3d)), while the middle of the left-hand edge of the rectangle represents the experiment in Figure 3e. The region outside this rectangle shows that moderately larger changes in wave climates would cause somewhat larger shoreline-change rates.

4. Discussion

[20] The rates of change in the numerical model involve some uncertainty. The empirical coefficient, K_1 , in equation 1 should in principle be calibrated for each shoreline. In the absence of appropriate measurements of alongshore flux or shoreline-change rates, a traditional value is often used, based on a fit to previous measurements [Komar, 1998]. For significant wave heights, as reported by the Wave Information Study (WIS) which we base our wave climates on, this traditional value corresponds to $K_1 = 0.17 \text{ m}^{1/2}/\text{s}$. However, we use a value of $K_1 = 0.4 \text{ m}^{1/2}/\text{s}$, calibrated to shoreline change rates on the Carolina coastline in the following way. Figure 3b shows that the strongest shoreline-change signals in the model, under the constant wave climate, are associated with cape tip migration. Erosion (accretion) rates just updrift (downdrift) of Cape Hatteras have been approximately 2 m/yr (3 m/yr) over the last half century (NC50). (Erosion rates just updrift of Cape Lookout are approximately the same as those at Cape Hatteras (NC50). Anthropogenic influences downdrift of Cape Lookout, and at Cape Fear, are too significant to use the data from those areas.) Using $K_1 = 0.4 \text{ m}^{1/2}/\text{s}$, the model reproduces these rates under the constant-wave-climate scenario.

[21] Along with gradients in alongshore sediment flux, sea-level rise and consequent cross-shore transport also tends to cause shoreline change. Assuming that the cross-shore

profile shape of the nearshore seabed (the ‘shoreface’) and sub-aerial barrier are maintained by wave action and remain constant over time, local conservation of mass dictates how far landward this composite profile will tend to shift for a given amount of sea-level rise [Cowell *et al.*, 1995; Bruun, 1962]. Because of the geometric assumptions of a low-slope, concave profile this conceptual framework makes, the rate of shoreline retreat is highly sensitive to the estimate of the depth limit of significant wave action. Nonetheless, some sea-level rise related retreat can be expected to be superimposed on the (generally much greater [Cowell *et al.*, 1995]) shoreline changes from gradients in alongshore transport. Researchers have suggested that this retreat rate can be roughly related to the rate of sea-level rise by multiplying the later by 100—a common but crude conversion that involves an assumed average slope to the shoreface profile of 1/100 [Zhang *et al.*, 2000, 2004; Dean and Maurmeyer, 1983]. With a 0.48 meter/century sea-level rise [IPCC, 2001] this would predict a resulting erosion rate of 0.48 meter/year—roughly an order of magnitude smaller than the increase in alongshore-averaged shoreline change rates for eroding areas caused by changing storm patterns in model scenarios (Figure 3).

[22] The highly simplified model considers gradients in alongshore sediment flux, leaving out various other processes that cause shoreline change in nature. In addition, the model scenarios involve unrealistic sudden shifts in wave climates; the results in Figures 3 and 4 should not be considered quantitatively reliable predictions. However, the model experiments show that shifts in coastline shape should be expected on complex-shaped coastlines, including parts of the US Southeast and Gulf coastlines and the northwest Alaska coast. (Where a predominance of low-angle waves in the regional wave climate has created smooth coastlines on the large scale, such as the Texas Gulf Coast, USA, possible changes in wave-climate asymmetry and net sediment transport could cause more subtle realignments of shoreline orientation.)

[23] Scientists and coastal managers, concentrating on the effects of sea-level rise, have implicitly assumed that the

shoreline response to global warming will be alongshore uniform [Cowell *et al.*, 1995; Bruun, 1962]. The initial results presented here suggest that coastal management strategies should not be based on this assumption. In addition, although the destructive potential of individual hurricane landfalls in the global warming context is certainly a concern, these model results suggest that the cumulative effects of changing storm patterns could also significantly impact coastal communities—causing coastline changes at least commensurate with those from sea-level rise. Figure 3 suggests that, while the particular pattern of shoreline changes depends on the scenario of storm-pattern changes, shoreline erosion in the future may be concentrated in areas very different than in the recent past (Figures 3d and 3e). Further modeling and observation of climate change and shoreline responses will lead to more specific predictions that should facilitate better preparation for future changes in the economically and ecologically important shoreline environment.

[24] **Acknowledgment.** The Andrew W. Mellon Foundation, the National Science Foundation Biocomplexity Program, and the Duke University Center on Global Change supported this work.

References

- Anderson, J., A. Rodrigues, C. Fletcher, and D. Fitzgerald (2001), Researchers focus attention on coastal response to climate change, *Eos Trans. AGU*, *82*, 513–520.
- Ashton, A. D., and A. B. Murray (2006a), High-angle-wave instability and emergent shoreline shapes: 1. Modeling of sandwaves, flying spits, and capes, *J. Geophys. Res.*, doi:10.1029/2005JF000422, in press.
- Ashton, A. D., and A. B. Murray (2006b), High-angle-wave instability and emergent shoreline shapes: 2. Wave climate analysis and comparisons to nature, *J. Geophys. Res.*, doi:10.1029/2005JF000423, in press.
- Ashton, A., A. B. Murray, and O. Arnault (2001), Formation of coastline features by large-scale instabilities induced by high-angle waves, *Nature*, *414*, 296–300.
- Ashton, A., J. H. List, A. B. Murray, and A. S. Farris (2003a), Links between erosional hotspots and alongshore sediment transport, in *Coastal Sediments '03: Annual Symposium on Coastal Engineering and Science of Coastal Sediment Processes* [CD-ROM], World Sci., Hackensack, N. J.
- Ashton, A., A. B. Murray, and G. B. Ruessink (2003b), Initial tests of a possible explanation for alongshore sandwaves on the Dutch Coast, in *Third International Symposium on River, Coastal and Estuarine Morphodynamics*, pp. 320–330, Int. Assoc. for Hydraul. Res., Barcelona.
- Brown, K., R. Few, E. L. Tompkins, M. Tsimplis, and S. Tarja (2004), Responding to climate change: Inclusive and integrated coastal analysis, *Tech. Rep. 24*, Tyndall Cent. for Clim. Change Res., Univ. of East Anglia, Norwich, U.K.
- Bruun, P. (1962), Coastal erosion and the development of beach profiles, *J. Waterw. Harbors Div. Am. Soc. Civ. Eng.*, *88*, 117–130.
- Cowell, P. J., P. S. Roy, and R. Jones (1995), Simulation of large-scale coastal change using a morphological behavior model, *Mar. Geol.*, *126*, 45–61.
- Dean, R. G., and E. M. Maurmeyer (1983), Models for beach profile response, in *CRC Handbook of Coastal Processes and Erosion*, edited by P. D. Komar and J. Moore, pp. 151–165, CRC Press, Boca Raton, Fla.
- Emanuel, K. A. (1987), The dependence of hurricane intensity on climate, *Nature*, *326*, 483–485.
- Emanuel, K. A. (2005), Increasing destructiveness of tropical cyclones over the past 30 years, *Nature*, *436*, 686–688.
- Geng, Q., and M. Sugi (2003), Possible change of extratropical cyclone activity due to enhanced greenhouse gases and sulfate aerosols—Study with a high resolution GCM, *J. Clim.*, *16*, 2802–2805.
- Gornitz, V. (1991), Global coastal hazards from future sea-level rise, *Global Planet. Change*, *89*, 379–398.
- Intergovernmental Panel on Climate Change (2001), *Climate Change 2001: Impact, Adaptation, and Vulnerability—Contribution of Working Group II to the Third Assessment Report of the Intergovernmental Panel on Climate Change*, Cambridge Univ. Press, New York.
- Komar, P. D. (1998), *Beach Processes and Sedimentation*, Simon and Schuster, Upper Saddle River, N. J.
- Komar, P. D., and D. L. Inman (1970), Longshore sand transport on beaches, *J. Geophys. Res.*, *75*, 5914–5927.
- Lambert, S. J. (1995), The effect of enhanced greenhouse warming on winter cyclone frequency and strengths, *J. Clim.*, *8*, 1447–1452.
- Murray, A. B., and A. Ashton (2004), Extending a 1-line modeling approach to explore emergent coastline behaviors, in *Coastal Engineering 2004* [CD-ROM], World Sci., Hackensack, N. J.
- Pilkey, O. H., W. J. Neal, S. R. Riggs, C. A. Webb, D. M. Bush, D. F. Pilkey, J. Bullock, and B. A. Cowan (1998), *The North Carolina Shore and Its Barrier Islands*, Duke Univ. Press, Durham, N. C.
- Titus, G. T., R. A. Park, S. P. Leatherman, J. R. Weggel, M. S. Greene, P. W. Mausell, S. Brown, G. Gaunt, M. Trehan, and G. Yohe (1991), Greenhouse effect and sea level rise: The cost of holding back the sea, *Coastal Manage.*, *19*, 171–204.
- Webster, P. J., G. J. Holland, J. A. Curry, and H.-R. Chang (2005), Changes in tropical cyclone number, duration, and intensity in a warming environment, *Science*, *309*, 1844–1846.
- Zhang, K. Q., B. C. Douglas, and S. P. Leatherman (2000), Twentieth-century storm activity along the U.S. east coast, *J. Clim.*, *13*, 1748–1761.
- Zhang, K. Q., B. C. Douglas, and S. P. Leatherman (2004), Global warming and coastal erosion, *Clim. Change*, *64*, 41–58.
- A. D. Ashton, Woods Hole Oceanographic Institution, MS-22, Woods Hole, MA 02543, USA.
- T. J. Crowley, A. B. Murray, and J. M. Slott, Division of Earth and Ocean Sciences, Nicholas School of the Environment and Earth Sciences, Center for Nonlinear and Complex Systems, Duke University, Box 90229, Durham, NC 27708-0227, USA. (jordan.slott@duke.edu)